Published in final edited form as:
Cancer Lett. 2013 October 28; 340(1): 63–71. doi:10.1016/j.canlet.2013.06.026.

An endogenous aryl hydrocarbon receptor ligand inhibits proliferation and migration of human ovarian cancer cells

Kai Wang[#a,b], **Yan Li**[#b], **Yi-Zhou Jiang**[b], **Cai-Feng Dai**[b,c], **Manish S. Patankar**[b], **Jia-Sheng Song**[d], and **Jing Zheng**[b,e,*]

[a]Shanghai First Maternity and Infant Hospital, Tongji University School of Medicine, Shanghai 200040, PR China

[b]Department of Obstetrics and Gynecology, University of Wisconsin, Madison, WI 53715, United States

[c]Qilu Hospital of Shandong University, Jinan 250012, Shandong, PR China

[d]AhR Pharmaceuticals, Inc., Madison, WI 53719, United States

[e]Department of Cardiovascular Medicine, Affiliated Hospital of Guangdong Medical College, Zhanjiang 524001, Guangdong, PR China

[#] These authors contributed equally to this work.

Abstract

The aryl hydrocarbon receptor (AhR), a ligand-activated transcription factor mediates many biological processes. Herein, we investigated if 2-(1′H-indole-3′-carbonyl)-thiazole-4-carboxylic acid methyl ester (ITE, an endogenous AhR ligand) regulated proliferation and migration of human ovarian cancer cells via AhR. We found that AhR was widely present in many histotypes of ovarian cancer tissues. ITE suppressed OVCAR-3 cell proliferation and SKOV-3 cell migration *in vitro*, which were blocked by AhR knockdown. ITE also suppressed OVCAR-3 cell growth in mice. These data suggest that the ITE might potentially be used for therapeutic intervention for at least a subset of human ovarian cancer.

Keywords

ITE; Aryl hydrocarbon receptor; Ovarian cancer cells; Growth

1. Introduction

To date, ovarian cancer is still the most lethal female genital cancer, largely because cancer cells acquire a chemoresistant phenotype after initial cytoreductive surgery and chemotherapy in the majority of cases [1,2]. Another major challenge of current cancer therapies is severe side effects and toxicity of chemotherapy drugs used. Thus, since human ovarian cancer is characterized by its high degree of heterogeneity at the cellular and molecular levels, understanding individual type of ovarian cancer is critical to develop an efficacious, but low side-effect cancer therapy [1,2].

[*]Corresponding author. Address: Department of Obstetrics and Gynecology, University of Wisconsin, PAB1 Meriter Hospital, 202 S. Park St., Madison, WI 53715, United States. Tel.: +1 (608) 417 6314; fax: +1 (608) 257 1304. jzheng@wisc.edu (J. Zheng)..

Disclosure statement

Dr. Jia-Sheng Song, PhD., is a major stakeholder and Chief Scientific Officer of the AhR Pharmaceuticals, Inc.

The aryl hydrocarbon receptor (AhR) is a ligand-activated transcriptional factor [3]. A classic AhR ligand is 2,3,7,8-tetrachlo-rodibenzo-*p*-dioxin (TCDD), which is a potent environmental toxicant and carcinogen [3]. The AhR mediated biological action is well known to involve a multi-step signal transduction process. Specifically, upon binding to its ligand and dissociation from its associated proteins, AhR translocates from the cytoplasm into the nucleus and dimerizes with AhR nuclear translocator (ARNT), activating a series of downstream genes (e.g., enzyme cytochrome P450 [CYP], family 1, member A1 and B1 [CYP1A1 and CYP1B1]), ultimately initiating the xenobiotic metabolizing process [3]. Once the metabolizing process is initiated, AhR in the nucleus transports back to the cytoplasm, in which AhR is degraded by the 26S proteasome system [4]. To date, it is well established that besides its participations in metabolizing xenobiotics, AhR also mediates a variety of other biological processes such as normal ovarian growth and function as evidenced by the fact that either AhR knockdown in mice or exposure to TCDD in rats could decrease the number of pre-antral and antral follicles and reduce or block ovulation [5-7].

The AhR ligand also can adversely impact estrogen receptor (ER) signaling directly via binding to ER target gene promoters [8] or indirectly via regulating the CYP family (e.g., CYP1A1 and CYP1B1) [9], which is also the key enzyme for estrogen metabolism. Thus, the AhR signaling could potentially affect behaviors of those estrogen-sensitive cells such as ovarian cancer cells [9], even though estrogen may differently regulate ovarian cancer cell growth, plausibly depending on individual subtypes of ovarian cancer, concentrations of estrogen, and patients' ages (e.g., pre- vs. post-menopause) [1,10].

The reports on potential roles of AhR in human cancer are controversial. Epidemiological studies have suggested that occupational exposures to high levels of TCDD did not increase risk of human ovarian cancer and endometriosis [11]; however, such exposures could be associated with a decreased risk in breast and endometrial cancers [12,13] and with an increased mortality from other cancer sites (e.g., lung cancer in men) [11-15]. Paradoxically, levels of AhR expression may not be positively correlated with the incidences of these cancers as the increased AhR expression has been reported in human breast and lung cancers [15,16]. Moreover, AhR gene polymorphisms are also closely associated with an increased risk of lung and breast cancers [16,17]. Nonetheless, AhR activation has been reported to suppress growth of breast, pancreatic, and liver cancers [15,18-20]. To date, little is known regarding the role of AhR in human ovarian cancer [20,21], although TCDD has been shown to stimulate proliferation of CAOV-3 cells, a human ovarian cancer cell line [21], suggesting that AhR could be used as a therapeutic target for treating ovarian cancer.

Many endogenous AhR ligands have been discovered [22], including 2-(1′H-indole-3′-carbonyl)-thiazole-4-carboxylic acid methyl ester (ITE), which was first isolated from porcine lungs [23]. Based on its activity on the dioxin responsive element, the biological potency of ITE was ~ 100-fold lower than that of TCDD [23]. Moreover, the estimated Kd value for ITE in mouse hepatoma cells was ~5-6-fold greater than that of TCDD [23]. However, given its naturally producing feature and specific binding to AhR [23], ITE could potentially be used for interfering ovarian cancer growth, particularly because of its lack of toxicity (e.g., cleft palate and hydronephrosis, which typically associated with perinatal TCDD exposure in the mouse fetus) [24,25].

To date, the roles of AhR in human ovarian cancer are poorly understood, and it is also unknown if activation of AhR by its endogenous ligand can affect ovarian cancer growth. Thus, given that the AhR signaling has been shown to suppress growth of breast, pancreatic, and liver cancers[12,15-17], in this study, we tested the hypothesis that the AhR activation by its endogenous ligand inhibited human ovarian cancer progress via attenuating growth

and/or migration of human ovarian cancer cells. We first determined AhR expression in human ovarian tissues and then examined if ITE regulated ovarian cancer cell proliferation and migration via AhR using *in vitro* and/or *in vivo* models.

2. Materials and methods

2.1. Immunohistochemistry

Immunolocalization of AhR was performed using the human ovarian cancer tissue microarray (US Biomax, Rockville, MD) as described [26,27]. This microarray contained 192 cases of ovarian cancer, 8 adjacent normal ovarian tissues, and 8 normal ovarian tissues. Major cancer histotypes include adult granular cell tumor (AGCT; $n = 4$), disgerminoma (DISG; $n = 5$), adenocarcinoma (ADEN; $n = 8$), teratoma malignant change (TMC; $n = 5$), yolk sac tumor (YST; $n = 6$), mucinous adenocarcinoma (Mu-ADEN; $n = 20$), and serous adenocarcinoma (Se-ADEN; n = 136), in which 21 were classified as the low grade (L-Se-ADEN) and 115 as the high grade (H-Se-ADEN) as described [28]. The pathologists widely used this morphology-based classification to classify ovarian cancer into major subgroups based on type of differentiation (e.g., serous, mucinous or endometrioid) and degree (tumor grade) [29,30]. Two microarrays were run in parallel: one was probed with a rabbit AhR antibody (2 μg/mL; Biomol International, Plymouth, PA)[27], and another was probed with preimmune rabbit IgG (2 μg/mL; as the control). The AhR immunoreactivity was visualized using the avidin–biotin complex kit with amino ethyl carbazol as a chromogen (Vector Laboratories, Burlingame, CA). Since no epithelial cells were detected on the surface of any normal ovarian tissue sections pre-sent in the tissue microarray, presumably due to the tissue collection and/or section procedure, we also performed immunohistochemical staining on tissue sections from one human normal ovary (kindly provided by Dr. Sana Salih, Department. of Ob/Gyn, University of Wisconsin–Madison) which contained epithelial cells on the surface of the ovary to determine presence of AhR in these cells.

To semi-quantitatively analyze the AhR levels, images from each histotype of tissue with $n \geq 4$ were taken as described [26,27]. The optical density (OD) values determined by using the NIH Image J analysis software were corrected from the preimmune rabbit IgG control for each corresponding tissue section. Since no difference in the OD values was observed between adjacent normal ovarian tissues and normal ovarian tissues, data from these two tissues were pooled.

2.2. Cell lines

Two human ovarian adenocarcinoma cell lines (SKOV-3 and OVCAR-3 from American Type Culture Collection, Manassas, VA) and a human immortalized ovarian surface epithelial (IOSE-385) cell line was kindly provided by Dr. Nelly Auersperg of the Canadian Ovarian Tissue Bank (University of British Columbia, Vancouver, Canada). Both cancer cell lines were isolated from ascites fluid and were classified as cisplatin-resistant [31]. However, these cancer cells differ in many other aspects. For example, while both OVCAR-3 and SKOV-3 cells are p53 defected [31], OVCAR-3, but not SKOV-3 cells express CA125 (a major ovarian cancer biomarker) [1] and respond to estrogen even though both express estrogen receptor (ER) and [2,32]. Thus, these cancer cell lines may represent cisplatin-resistant cohorts of patients with ovarian cancer cells which are different in the expression of CA125, and in the response to estrogen. SKOV-3 and IOSE-385 cells were cultured in RPMI 1640 medium (Invitrogen, Carlsbad, CA) containing 10% FBS, penicillin/streptomycin (designed as the complete growth media). OVCAR-3 cells were cultured in the complete media supplemented with 10 μg/mL insulin (Sigma–Aldrich, St. Louis, MO).

2.3. Cell proliferation and migration assays

Cell proliferation was assayed as described [33,34]. After 16 h (Day 0) of seeding in 96-well plates (1000, 5000, and 5000 cells/well for SKOV-3, OVCAR-3, and IOSE-385, respectively; 6 wells/dose), cells were treated with different concentration of ITE (0.1–5000 nM, Tocris Bioscience, San Diego, CA) or DMSO (0.1% v/v) in the complete growth media up to 6 days with daily change of media containing dimethyl sulfoxide (DMSO, the vehicle control) or ITE. At the end of treatment, the number of cells per well was determined using a crystal violet method as described [33,34]. Briefly, after treatment, cells were rinsed with PBS (5 mM phosphate, 145 mM NaCl, 5 mM KCl, pH 7.5), fixed in methanol for 15 min, air-dried for 5 min and stained with 0.1% (w/v) crystal violet for 5 min. After staining, wells were rinsed with distilled water, and air dried again. Once dry, cells were solubilized with 2% (w/v) sodium deoxycholate solution for 30 min with gentle agitation. Absorbance was measured at 570 nm on a microplate reader. Wells containing known cell numbers (0, 2500, 5000, 10,000 and 20,000 cells/well; $n = 6$/cell density) were treated in the similar fashion to establish standard curves for each individual cell line.

Cell migration was evaluated using a FluoroBlok Insert System (8.0 μm pores; BD Biosciences, San Jose, CA) as described [26]. Since OVCAR-3 cells do not migrate in this system as we reported recently [26], OVCAR-3 cells were not assayed. After reaching 70–80% confluence, cells grown on 60 mm culture dishes were treated with 1 μM of ITE in the complete growth media for 6, 4, 2 or 0 days with a daily change of media containing DMSO or ITE. Cells were lifted on the same day using trypsin and were seeded into the insert (30,000 cells/insert). Cells were cultured in the same media containing DMSO or ITE (the exact same media in the upper and bottom wells). After 16 h, cells migrated were stained with 0.2 g/mL of calcein AM (Invitrogen) and counted using the MetaMorph image analysis software.

2.4. Western blot analysis

Western blot analysis was conducted as described [26,27]. Subconfluent cells were treated with a single dose of ITE (1 μM) in the complete growth media for 48, 24, 8, 2, 1, or 0 h. Proteins (20 μg for AhR and 40 μg for the CYP1A1) were subjected to Western blotting. The membranes were probed with the rabbit anti-AhR (1: 2000; Biomol International) [27] or a mouse monoclonal anti-CYP1A1 antibody (1:1000; Oxford Biomedical Research, Oxford, MI) [35], followed by reprobing with a rabbit GAPDH (Glyceraldehyde 3-phosphate dehydrogenase) antibody (1:10,000; Research Diagnostics, Concord, MA). Proteins were visualized using the enhanced chemiluminescence reagent (Amersham, Piscataway, NJ).

2.5. RNA isolation and real-time PCR

Subconfluent cells were treated with a single dose of ITE (1 μM) in the complete growth media for 24, 8, 2, 1, or 0 h. Total RNA were extracted using Trizol and RNA simple Total RNA Kit (Tiangen Biotech, Beijing, China) and quantified by using a spectrophotometer. Samples of total RNA from each treatment (1 μg) were reverse transcribed to cDNA. The reverse transcription (RT) was carried out using PrimeScript RT reagent Kit (TaKaRa, Dalian, China) for 15 min at 37 °C, 5s at 85 °C in a 20 μl reaction volume. Real-time PCR was performed using SYBR Premix Ex Taq (TaKaRa) according to the manufacturer's instruction. Primers for GAPDH (Sense: 5′-GCACCGTCAAGGCTGAGAAC-3′; Antisense: 5′-TGGTGAAGACGC-CAGTGGA-3′) and CYP1A1 (Sense: 5′-CACAGCACAACAAGAGAC-ACAA-3′; Antisense: 5′-TAGCCAGGAAGAGAAAGACCTC-3′) were synthesized (Sangon Biotechnology, Shanghai, China). The realtime PCR reaction was carried out at 30 s at 95 °C for incubation, and then 15 s at 95 °C and 20 s at 56 °C for 40 cycles. To confirm the amplification

specificity, the PCR products were subjected to a melting curve analysis. Levels of mRNA were analyzed using 2-ΔΔCT method.

2.6. siRNA transfection

Transfection of siRNA was performed as described [33,34]. The AhR siRNA target human AhR was purchased (Dharmacon, Chicago, IL; Cat # L-004990-00-0020). Two scrambled siRNA (siRNA controls) with 5′- Cy3 were synthesized (IDT, Coralville, IW): one (Sense: 5′-AGUUUGACCUGCUCUCCAUTT-3′; Antisense: 3′-TTUCAAACUGGACGAGAGGUA-5′) was used for SKOV-3 cells, and the other (Sense: 5′-GAGAGGUCCCUCCCAUCUUTT-3′; Antisense: 5′-AAGAUGGGAGGGACCUCUCTT-3′) for OVCAR-3 cells. Subconfluent cells were transfected with the AhR siRNA or scrambled siRNA in the Lipofectamine RNAiMAX transfection reagent (Invitrogen) or treated with the Lipofectamine RNAiMAX transfection reagent alone (the vehicle control) up to 6 days. After an optimal dose and time point were identified, additional cells were transfected for determining their proliferative or migrative responses to ITE.

2.7. Mouse xenograft models

To confirm anti-cancer action of ITE *in vivo*, female BALB/c nude mice (6–8 weeks of age and weighed 18–22 grams) were used as described [36]. The animal studies were approved and performed by Crown Bioscience, Inc. (Santa Clara, CA), following guidelines approved by the Institutional Animal Care and Use Committee of Crown Bioscience, based on the guidance of the Association for Assessment and Accreditation of Laboratory Animal Care.

OVCAR-3 cells at 70–80% confluence were harvested. Each mouse was inoculated subcutaneously at the right flank with 5×10^6 of OVCAR-3 cells. When the tumor volume reached approximately 110 mm^3, the mice were divided into homogeneous blocks based on their tumor volumes followed by randomly assigning each block into the vehicle control and ITE treatment groups ($n = 8$/group). The vehicle (DMSO) or ITE (80 mg/mL in DMSO, KNC Laboratories Co., Ltd., Tokyo, Japan) was administered to the mice by i.p. injection once daily for 28 days at a volume of 1 mL/kg body weight. After the final injection, mice were given an additional 5 days to further monitor tumor volume, body weight, and other clinical signs [36].

A gross body weight and tumor volume were determined twice weekly, the latter of which was measured using a caliper expressed in mm^3 as described [36]. Tumor weights were converted from tumor volumes by assuming a tumor density of 1 mm^3= 1 mg. A net body weight was obtained by subtracting a tumor weight from a gross body weight.

2.8. Statistics

Data were analyzed using one-way ANOVA using the SigmaStat software (Jandel Co., San Rafael, CA). When an *F*-test was significant, data were compared with their respective control by the Bonferroni's multiple comparison test or Student *t*-test. $p \leq 0.05$ was considered statistically significant. The IC50 value for ITE-inhibited OVCAR-3 cell proliferation was estimated using an Origin data analysis and graphing software (Version 8.1) (OriginLab Corporation Northampton, MA).

3. Results

3.1. AhR immunolocalization

In the ovarian cancer tissue microarray, the AhR immunoreactivity was present in DISG, ADEN, TMC, YST, Mu-ADEN, and L- and H-Se-ADEN, but not in NORM (*Note*: no

epithelial cells were seen on the surface of all 16 NORM cases in this tissue microarray) and AGCT (Fig. 1A). In Mu-ADEN and Se-ADEN, the AhR staining was localized primarily in epithelial cells, but not other cell types. No positive staining was observed in the preimmune rabbit IgG (data not shown). The positive AhR staining was clearly present in surface epithelia of a human normal ovary which was locally obtained (Fig. 1A-j). Thus, the positive AhR expression in IOSE-385, derived from human ovarian surface epithelial cells, was not surprising. The semi-quantification analysis revealed that the OD value in NORM was similar to that in DISG and ADEN, but was much lower ($p \leq 0.05$) than that in TMC, YST, Mu-ADEN, and L- and H-Se-ADEN (Fig. 1B). No difference was detected between the grades, stages, and TNM classifications in each histotype of ovarian cancer tissues studied (data not shown).

3.2. ITE inhibits ovarian cancer cell proliferation and migration

As compared to the vehicle control, ITE dose- and time-dependently inhibited ($p \leq 0.05$) OVCAR-3 (Fig. 2), but not SKOV-3 and IOSE-385 cell proliferation (not shown). The maximal inhibitory effect of ITE on OVCAR-3 cell proliferation was observed at doses from 10 nM to 5000 nM on Day 6 (Fig. 2). The estimated IC_{50} of ITE for OVCAR-3 cell proliferation on Day 6 was 0.21 nM. Moreover, treatment with ITE for 6, 4, and 2 days similarly inhibited ($p \leq 0.05$) SKOV-3 by ~54% (Fig. 3B), but not IOSE-385 cell migration (Fig. 3B).

3.3. ITE decreases AhR and increases CYP1A1 level

The AhR protein was detected in all three cell lines at ~95 kD (Fig. 4A) as reported [27,37]. A single dose of ITE (1 μM) significantly decreased ($p \leq 0.05$) AhR protein levels in SKOV-3, OVCAR-3, and IOSE-385 cells (Fig. 4A), indicating AhR activation [4]. However, the patterns of changes in AhR protein levels were quite different among these three cell cells (Fig. 4A). For example, the ITE-induced decrease in AhR began at 2 h, lasted up to 8 h and then increased in SKOV-3 cells, whereas such a decrease started at 1 h and maintained up to 48 h in OVCAR-3 and IOSE-385 cells (Fig. 4A). A single dose of ITE also time-dependently increased ($p \leq 0.05$) CYP1A1 protein levels in SKOV-3 (~5-fold) and OVCAR-3 (~3-fold), but not in IOSE-385 cells, beginning at 24 h and maintaining at this relatively high level up to 48 h (Fig. 4A).

To confirm ITE-increased CYP1A1 expression in SKOV-3 and OVCAR-3 cells, real time PCR was performed (Fig. 4B). Consistently with Western blot analysis, real time PCR revealed that ITE increased ($p \leq 0.05$) CYP1A1 mRNA levels in both SKOV-3 (~3.1 and 3.7-fold at 2 and 8 h, respectively) and OVCAR-3 (~3-fold at 8 h) cells (Fig. 4B), indicating that ITE indeed induced CYP1A1 expression.

3.4. AhR knockdown blocks ite-suppressed ovarian cancer cell proliferation and migration

As compared with the transfection reagent (the vehicle control) and the scrambled siRNA (the siRNA control), the AhR siRNA at 20 and 40 nM similarly decreased ($p \leq 0.05$) AhR protein levels in SKOV-3 by ~95%, 88%, and 76% on Days 2, 4, and 6, respectively (Fig. 5A). The AhR siRNA at 20 nM reduced ($p \leq 0.05$) AhR protein levels in OVCAR-3 by ~97%, 96%, and 86% on Days 2, 4, and 6,respectively (Fig. 5A). Importantly, AhR knockdown blocked ($p \leq 0.05$) ITE-suppressed OVCAR-3 cell proliferation and SKOV-3 cell migration (Fig. 5B), indicating the AhR-dependent suppression. In addition, AhR knockdown did not affect OVCAR-3 cell proliferation and SKOV-3 cell migration in the absence of ITE (Fig. 5B).

3.5. ITE attenuates ovcar-3 xenograft growth

As compared to the vehicle (DMSO) control, ITE inhibited ($p \leq 0.05$) the growth of OVCAR-3 xenografts in mice, starting at Day 15 of treatment (39% deduction) and continuing up to Day 28 (48%) (Fig. 6A). This inhibitory effect maintained for at least another 5 days after ITE administration was terminated (50% on Days 29 and 33; Fig. 6A). As compared to the vehicle control, ITE treatment caused ($p \leq 0.05$) a net body weight loss on Day 4; however, the net body weight was rapidly regained after Day 8 and maintained at the similar level afterward (Fig. 6B), suggesting that the current regimen was well tolerated by mice. During the course of ITE and DMSO treatments, all animals survived without any visible side effects (not shown).

4. Discussion

Herein we have shown that (1) AhR is widely expressed in human cancer tissues; (2) ITE inhibits OVCAR-3 cell proliferation and SKOV-3 cell migration *in vitro via* AhR; and (3) ITE suppresses OVCAR-3 cell growth in mice without significant side effect. Thus, these data are the first as far as we are aware, to demonstrate that activation of the ITE/AhR suppresses ovarian cancer cell proliferation and/or migration, suggesting that ITE might potentially be used as a therapeutic drug for treating at least a subset of human ovarian cancer.

Our observations that AhR is expressed in a variety of histotypes of ovarian cancers regardless of cancer grades, stages, and TNM grading are consistent with the previous reports in human ovarian cancer [25] and in lung and breast cancers [13-16]. These data indicate broad expression of AhR in human epithelial cancer tissues, implying overall importance of AhR in all of these histotypes of ovarian cancer, even though that AhR may not be suitable to be used for predicting the severity of ovarian cancer. In addition, since the AhR staining is positive in surface epithelial cells, but negative inside the normal ovary, relatively high levels of AhR expression inside the ovary indicate the invagination of surface epithelial cells into the ovary in ovarian cancer, which could be used as one tissue marker for ovarian cancers as suggested previously [25].

It has been reported that in the absence of a ligand, AhR actually acts as a tumor suppressor in liver [19]. Similarly, an increase in invasiveness of breast cancer cells was also observed after the AhR knockdown [20]. In the current study, the AhR knockdown, however, does not alter SKOV-3 and OVCAR-3 cell proliferation and migration in the absence of ITE (Fig. 5), implying that AhR alone is unlikely to have significant impacts on ovarian cancer cell proliferation and migration. It, however, cannot be excluded that AhR might mediate cellular processes other than cell proliferation and migration in these ovarian cancer cells. For example, it would be interesting to investigate if AhR mediates chemoresistance of ovarian cancer cells as such mediation has been reported in human colorectal cancers [4].

In the current study, we demonstrate that ITE differentially mediates OVCAR-3, SKOV-3, and IOSE-385 cell proliferation and migration *in vitro*. For example, ITE inhibits OVCAR-3, but not SKOV-3 and IOSE-385 cell proliferation, while ITE suppresses SKOV-3, but not IOSE cell migration. The failure of IOSE-358 cells to respond to ITE implies that ITE may specifically target ovarian cancer cells, but not normal ovarian epithelial cells. Importantly, we further confirmed that ITE time-dependently suppressed growth of OVCAR-3 cell xenografts without a significant side effect on mice, which is in line with the previous reports showing that ITE has no significant fetotoxicity [24,25].

The mechanisms underlying differential mediations of AhR among these three cell lines studied require further investigation. However, it is noteworthy that the lack of the cell

proliferative and/or migrative response to ITE in these three cell lines obviously does not result from uncoupling ITE to AhR since ITE rapidly (≤8 h) decreased AhR protein levels (a hallmark of the AhR activation) in all three cell lines studied. Instead, the lack of these cell responses is possibly due to uncoupling activated AhR to its downstream signaling molecules such as CYP1A1 in IOSE-385 cells. In contrast, uncoupling AhR to CYP1A1 cannot explain such different mediations between OVCAR-3 and SKOV-3 cells. Thus, other yet to be identified signaling cascades must be involved in such different mediations of ITE between OVCAR-3 and SKOV-3 cells. These downstream signaling molecules could include other members of CYP family [2,3], although the direct link between CYP and these cell response remains to be established. These downstream signaling molecules could also include protein kinases such as the MAPK, AKT1, and FAK [38-40] as all of which are known to be critical for regulating cancer cell function. Alternatively, such differential mediations could due to the different expression and/or defect of steroid receptors such as ER in these two ovarian cancer cell lines [32], since ER has intricate interactions with AhR [41]. For instance, although both OVCAR-3 and SKOV-3 cells are ER-positive, a mutation in ER transcripts in SKOV-3 cells renders these cells insensitive to estrogen [2,32]. Thus, although it is possible that the ITE-inhibited OVCAR-3 cell proliferation could be mediated partially via interfering the ER signaling as ER could be activated by estrogen possibly present in serum used or phenol red (a weak estrogen analog) in the media used; however, such interference is unlikely to participate in the ITE-attenuated SKOV-3 cell migration.

It is noted that restoration of AhR levels after ITE treatment is much faster in SKOV-3 than OVCAR-3 cells (Fig. 4). Currently, it is unclear what cause these different restorations; however, it is possibly due to the different transcription and/or translation rates of AhR between SKOV-3 and OVCAR-3 cells upon AhR activation and degradation.

In summary, our current data from both in vitro and in vivo studies clearly demonstrate that ITE possesses potent anti-ovarian cancer activity dependent on AhR. Further dissecting out signaling pathways which mediate ITE-induced different cell responses between different ovarian cancer cells might assist us to design more optimal strategies for therapeutic intervention of human ovarian cancer, a highly heterogeneous disease.

Acknowledgments

This work was supported in part by the US National Institutes of Health Grant HD38843 (Magness/JZ) & the National Natural Science Foundation of China No. 81100429 (KW).

References

[1]. Bast RC, Hennessy B, Mills GB. The biology of ovarian cancer: new opportunities for translation. Nat. Rev. Cancer. 2009; 9:415–428. [PubMed: 19461667]

[2]. Yap TA, Carden CP, Kaye SB. Beyond chemotherapy: targeted therapies in ovarian cancer. Nat. Rev. Cancer. 2009; 9:167–181. [PubMed: 19238149]

[3]. Safe S, McDougal A. Mechanism of action and development of selective aryl hydrocarbon receptor modulators for treatment of hormone-dependent cancers. Int. J. Oncol. 2002; 20:1123–1128. [PubMed: 12011988]

[4]. Fujii-Kuriyama Y, Kawajiri K. Molecular mechanisms of the physiological functions of the aryl hydrocarbon (dioxin) receptor, a multifunctional regulator that senses and responds to environmental stimuli. Proc. Jpn. Acad. Ser. B. Phys. Biol. Sci. 2010; 86:40–53.

[5]. Clapp RW, Jacobs MM, Loechler EL. Environmental and occupational causes of cancer: new evidence 2005-2007. Rev. Environ. Health. 2008; 23:1–37. [PubMed: 18557596]

[6]. Diamanti-Kandarakis E, Bourguignon JP, Giudice LC, Hauser R, Prins GS, Soto AM, Zoeller RT, Gore AC. Endocrine-disrupting chemicals: an endocrine society scientific statement. Endocr. Rev. 2009; 30:242–293.

[7]. Hernandez-Ochoa I, Karman BN, Flaws JA. The role of the aryl hydrocarbon receptor in the female reproductive system. Biochem. Pharmacol. 2009; 77:547–559. [PubMed: 18977336]

[8]. Ahmed S, Valen E, Sandelin A, Matthews J. Dioxin increases the interaction between aryl hydrocarbon receptor and estrogen receptor alpha at human promoters. Toxicol. Sci. 2009; 111:254–266. [PubMed: 19574409]

[9]. Shanle EK, Xu W. Endocrine disrupting chemicals targeting estrogen receptor signaling: identification and mechanisms of action. Chem. Res. Toxicol. 2011; 24:6–19. [PubMed: 21053929]

[10]. Cunat S, Hoffmann P, Pujol P. Estrogens and epithelial ovarian cancer. Gynecol. Oncol. 2004; 94:25–32. [PubMed: 15262115]

[11]. Consonni D, Pesatori AC, Zocchetti C, Sindaco R, D'Oro LC, Rubagotti M, Bertazzi PA. Mortality in a population exposed to dioxin after the Seveso, Italy, accident in 1976: 25 years of follow-up. Am. J. Epidemiol. 2008; 167:847–858. [PubMed: 18192277]

[12]. Bertazzi PA, Zocchetti C, Guercilena S, Consonni D, Tironi A, Landi MT, Pesatori AC. Dioxin exposure and cancer risk: a 15-year mortality study after the "Seveso accident". Epidemiology. 1997; 8:646–652. [PubMed: 9345664]

[13]. Viel JF, Clement MC, Hagi M, Grandjean S, Challierl B, Danzon A. Dioxin emissions from a municipal solid waste incinerator and risk of invasive breast cancer: a population-based case-control study with GIS-derived exposure. Int. J. Health Geogr. 2008; 7:4. [PubMed: 18226215]

[14]. Lin P, Chang H, Tsai WT, Wu MH, Liao YS, Chen JT, Su JM. Overexpression of aryl hydrocarbon receptor in human lung carcinomas. Toxicol. Pathol. 2003; 31:22–30. [PubMed: 12597446]

[15]. Steenland K, Bertazzi P, Baccarelli A, Kogevinas M. Dioxin revisited: developments since the, 1997 IARC classification of dioxin as a human carcinogen. Environ. Health. Perspect. 2004; 112:1265–1268. [PubMed: 15345337]

[16]. Wong P, Li W, Vogel C, Matsumura F. Characterization of MCF mammary epithelial cells overexpressing the arylhydrocarbon receptor (AhR). BMC Cancer. 2009; 9:234. [PubMed: 19604390]

[17]. Kim JH, Kim H, Lee KY, Kang JW, Lee KH, Park SY, Yoon HI, Jheon SH, Sung SW, Hong YC. Aryl hydrocarbon receptor gene polymorphisms affect lung cancer risk. Lung Cancer. 2007; 56:9–15. [PubMed: 17174437]

[18]. Wormke M, Castro-Rivera E, Chen I, Safe S. Estrogen and aryl hydrocarbon receptor expression and crosstalk in human Ishikawa endometrial cancer cells. J. Steroid. Biochem. Mol. Biol. 2000; 72:197–207. [PubMed: 10822009]

[19]. Fan Y, Boivin GP, Knudsen ES, Nebert DW, Xia Y, Puga A. The aryl hydrocarbon receptor functions as a tumor suppressor of liver carcinogenesis. Cancer Res. 2010; 70:212–220. [PubMed: 19996281]

[20]. Hall JM, Barhoover MA, Kazmin D, McDonnell DP, Greenlee WF, Thomas RS. Activation of the aryl-hydrocarbon receptor inhibits invasive and metastatic features of human breast cancer cells and promotes breast cancer cell differentiation. Mol. Endocrinol. 2010; 24:359–369. [PubMed: 20032195]

[21]. Ouellet V, Guyot MC, Le Page C, Filali-Mouhim A, Lussier C, Tonin PN, Provencher DW, Mes-Masson AM. Tissue array analysis of expression microarray candidates identifies markers associated with tumor grade and outcome in serous epithelial ovarian cancer. Int. J. Cancer. 2006; 119:599–607. [PubMed: 16572426]

[22]. Nguyen LP, Bradfield CA. The search for endogenous activators of the aryl hydrocarbon receptor. Chem. Res. Toxicol. 2008; 21:102–116. [PubMed: 18076143]

[23]. Song J, Clagett-Dame M, Peterson RE, Hahn ME, Westler WM, Sicinski RR, DeLuca HF. A ligand for the aryl hydrocarbon receptor isolated from lung. Proc. Natl. Acad. Sci. USA. 2002; 99:14694–14699. [PubMed: 12409613]

[24]. Henry EC, Bemis JC, Henry O, Kende AS, Gasiewicz TA. A potential endogenous ligand for the aryl hydrocarbon receptor has potent agonist activity in vitro and in vivo. Arch. Biochem. Biophys. 2006; 450:67–77. [PubMed: 16545771]

[25]. Quintana FJ, Murugaiyan G, Farez MF, Mitsdoerffer M, Tukpah AM, Burns EJ, Weiner HL. From the Cover: an endogenous aryl hydrocarbon receptor ligand acts on dendritic cells and T cells to suppress experimental autoimmune encephalomyelitis. Proc. Natl. Acad. Sci. USA. 2010; 107:20768–20773. [PubMed: 21068375]

[26]. Dai C, Jiang YZ, Li Y, Wang K, Liu P, Patankar MS, Zheng J. Expression androles of Slit/Robo in human ovarian cancer. Histochem. Cell Biol. 2011; 135:475–485. [PubMed: 21465248]

[27]. Jiang YZ, Wang K, Fang R, Zheng J. Expression of aryl hydrocarbon receptor in human placentas and fetal tissues. J. Histochem. Cytochem. 2010; 58:679–686. [PubMed: 20354149]

[28]. Ayhan A, Kurman RJ, Yemelyanova A, Vang R, Logani S, Seidman JD, Shih IeM. Defining the cut point between low-grade and high-grade ovarian serous carcinomas: a clinicopathologic and molecular genetic analysis. Am. J. Surg. Pathol. 2009; 33:1220–1224. [PubMed: 19461510]

[29]. Soslow RA. Histologic subtypes of ovarian carcinoma: an overview. Int. J. Gynecol. Pathol. 2008; 27:161–174. [PubMed: 18317227]

[30]. McCluggage WG. Morphological subtypes of ovarian carcinoma: a review with emphasis on new developments and pathogenesis. Pathology. 2011; 43:420–432. [PubMed: 21716157]

[31]. Hagopian GS, Mills GB, Khokhar AR, Bast RC, Siddik ZH. Expression of p53 in cisplatin-resistant ovarian cancer cell lines: modulation with the novelplatinum analogue (1R, 2R-diaminocyclohexane) (trans-diacetato) (dichloro)platinum(IV). Clin. Cancer Res. 1999; 5:655–663. [PubMed: 10100719]

[32]. Lau KM, Mok SC, Ho SM. Expression of human estrogen receptor-alpha and-beta, progesterone receptor, and androgen receptor mRNA in normal and malignant ovarian epithelial cells. Proc. Natl. Acad. Sci. USA. 1999; 96:5722–5727. [PubMed: 10318951]

[33]. Song Y, Wang K, Chen DB, Magness RR, Zheng J. Suppression of protein phosphatase 2 differentially modulates VEGF- and FGF2-induced signaling in ovine fetoplacental artery endothelial cells. Placenta. 2009; 30:907–913. [PubMed: 19692121]

[34]. Wang K, Song Y, Chen DB, Zheng J. Protein phosphatase 3 differentially modulates vascular endothelial growth factor- and fibroblast growth factor 2-stimulated cell proliferation and signaling in ovine fetoplacental artery endothelial cells. Biol. Reprod. 2008; 79:704–710. [PubMed: 18509162]

[35]. Jobe SO, Ramadoss J, Koch JM, Jiang YZ, Zheng J, Magness RR. Estradiol-17beta and its cytochrome p450- and catechol-o-methyltransferase-derived metabolites stimulate proliferation in uterine artery endothelial cells: role of estrogen receptor-alpha versus estrogen receptor-beta. Hypertension. 2010; 55:1005–1011. [PubMed: 20212268]

[36]. Alley, MC.; Hollingshead, MG.; Dykes, DJ.; Waud, WR. Human tumor xegograft models in NCI drug development. In: Teicher, BA.; Andrew, PA., editors. Anticancer Drug Development Guide: Prelinical Screening, Clinical Trials, and Approval. Humana Press; Totowa: 2004. p. 125-152.

[37]. Juan SH, Lee JL, Ho PY, Lee YH, Lee WS WS. Antiproliferative and antiangiogenic effects of 3-methylcholanthrene, an aryl-hydrocarbon receptor agonist, in human umbilical vascular endothelial cells. Eur. J. Pharmacol. 2006; 530:1–8. [PubMed: 16359657]

[38]. Tan Z, Chang X, Puga A, Xia Y. Activation of mitogen-activated protein kinases (MAPKs) by aromatic hydrocarbons: role in the regulation of aryl hydrocarbon receptor (AHR) function. Biochem. Pharmacol. 2002; 64:771–780. [PubMed: 12213569]

[39]. Tan Z, Huang M, Puga A, Xia Y. A critical role for MAP kinases in the control of Ah receptor complex activity. Toxicol. Sci. 2004; 82:80–87. [PubMed: 15272135]

[40]. Wu R, Zhang L, Hoagland MS, Swanson HI. Lack of the aryl hydrocarbon receptor leads to impaired activation of AKT/protein kinase B and enhanced sensitivity to apoptosis induced via the intrinsic pathway. J. Pharmacol. Exp. Ther. 2007; 320:448–457. [PubMed: 17018692]

[41]. Ohtake F, Fujii-Kuriyama Y, Kawajiri K, Kato S. Cross-talk of dioxin and estrogen receptor signals through the ubiquitin system. J. Steroid. Biochem. Mol. Biol. 2011; 127:102–117. [PubMed: 21397018]

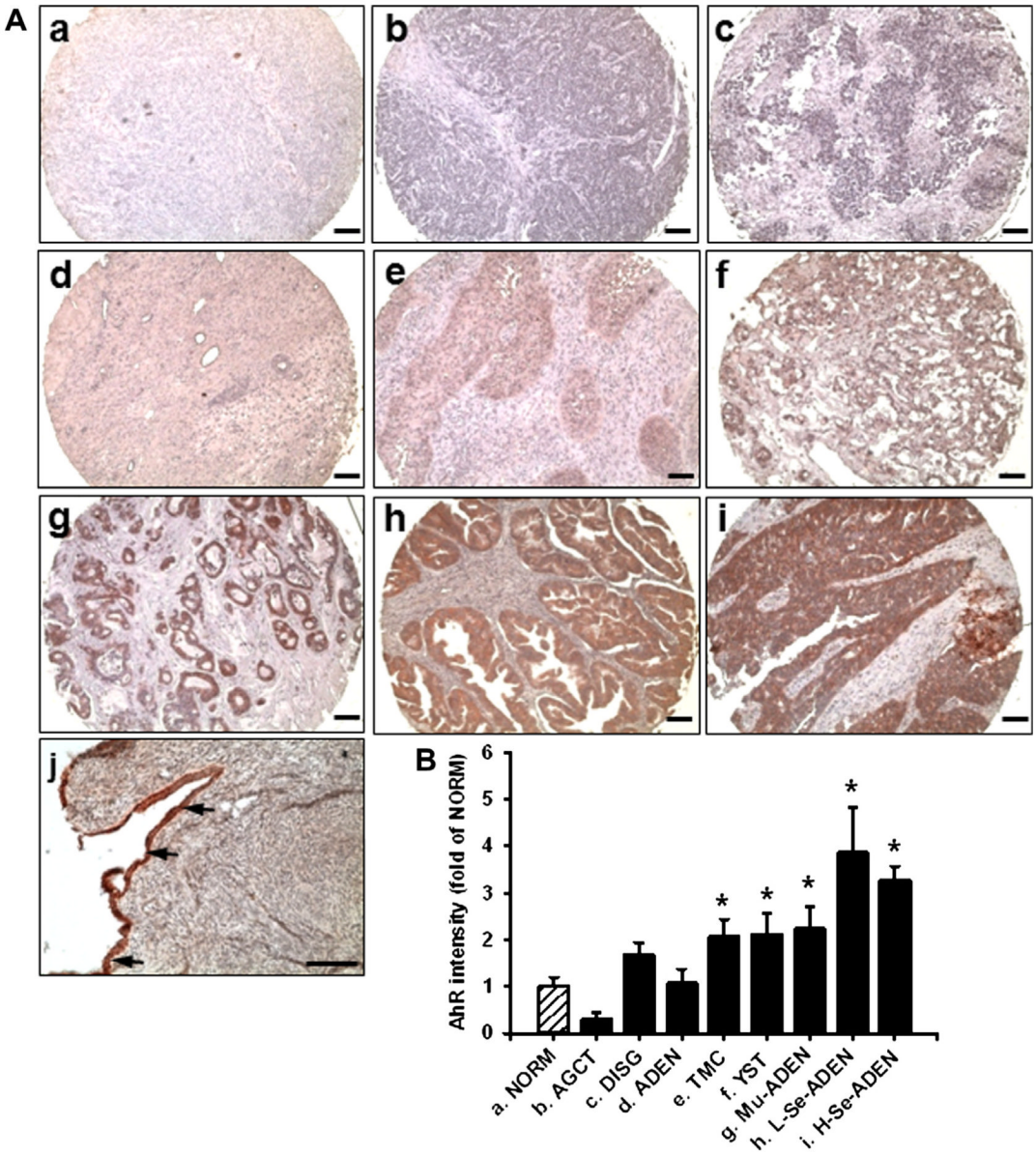

Fig. 1.

Immunohistochemical analysis for AhR in human ovarian cancer tissues and normal ovarian tissues. Reddish color indicates positive AhR staining. (A) Representative images from NORM (a), AGCT (b), DISG (c), ADEN (d), TMC (e), YST (f), Mu-SDEN (g), L-Se-ADEN (h), and H-Se-ADEN (i) are shown. (j) A human normal ovary obtained locally. Arrows: epithelial cells on the surface of an ovary. Bar, 100 μm. (B) Semi-quantitative analysis for AhR staining intensities for NORM ($n = 16$), AGCT ($n = 4$), DISG ($n = 5$), ADEN ($n = 8$), TMC ($n = 5$), YST ($n = 6$), Mu-ADEN ($n = 19$), L-Se-ADEN ($n = 21$) and H-Se-ADEN ($n = 115$). Semi-quantitative data are expressed as Means ± SEM fold of the OD value from NORM. *Differ from NORM ($p \leq 0.05$). (For interpretation of the references to color in this figure legend, the reader is referred to the web version of this article.)

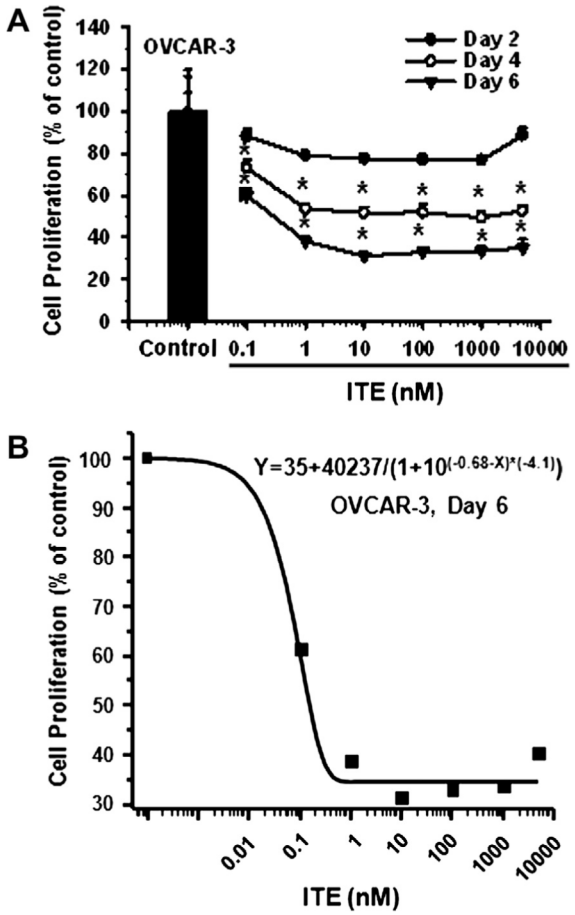

Fig. 2.

Effects of ITE on OVCAR-3 cell proliferation. Cells were treated without or with different doses of ITE up to 6 days. Cell proliferation is expressed as Means ± SEM% of the control (n = 3–4). *Differ from the control at each corresponding day ($p \leq 0.05$).

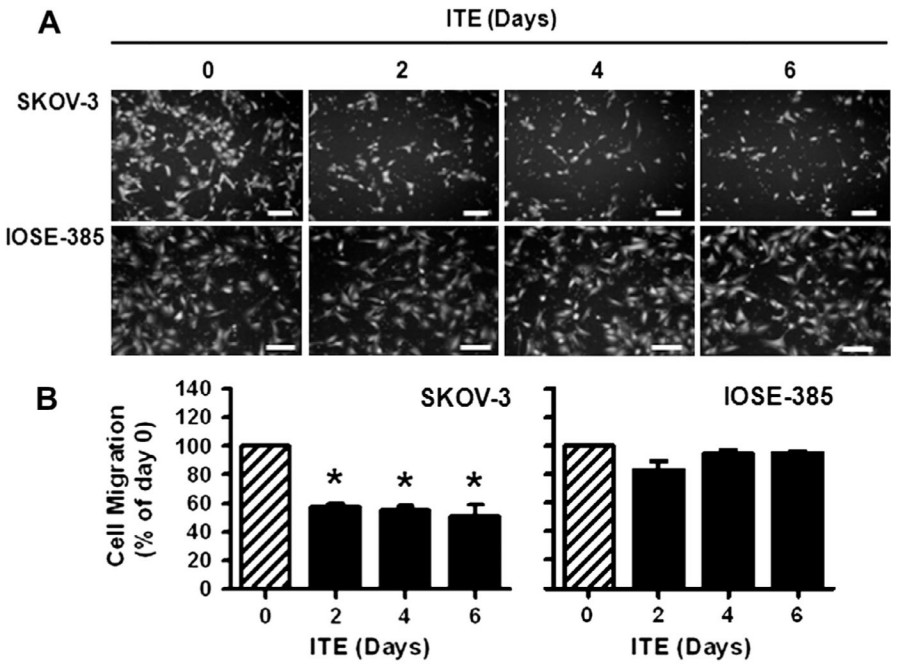

Fig. 3.

Effects of ITE on SKOV-3 and IOSE-358 cell migration. Cells were treated with ITE (1 μM) up to 6 days, followed by the migration assay. Cell numbers are expressed as Means ± SEM% of the Day 0 control ($n = 3$). *Differ from the Day 0 control ($p \leq 0.01$). Bars, 200 μm.

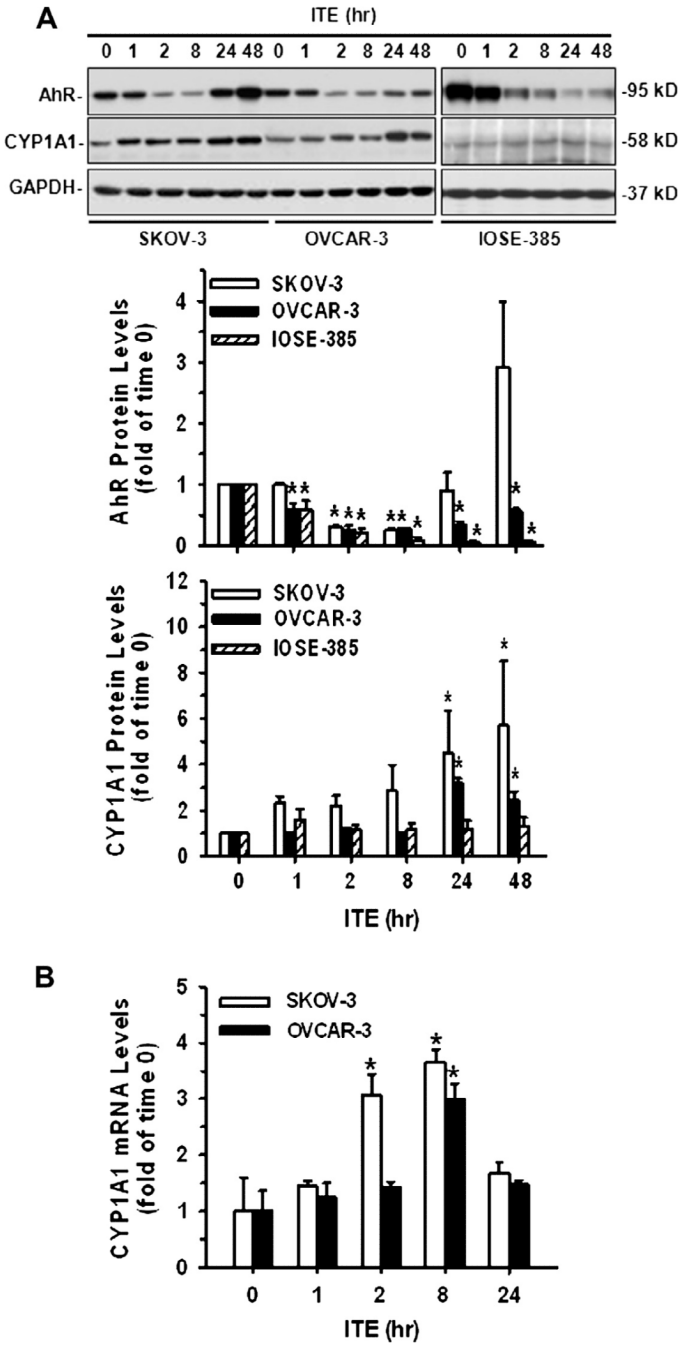

Fig. 4.

Effects of ITE on AhR and CYP1A1 expression in SKOV-3, OVCAR-3, and/or IOSE-385 cells. (A) Western blot analysis for AhR and CYP1A1 in SKOV-3, OVCAR-3, and IOSE-385 cells: Cells were treated with a single dose of ITE (1 μM) up to 48 h. Proteins were subjected to Western blotting. (B) Real time PCR analysis for CYP1A1 mRNA in SKOV-3 and OVCAR-3 cells: Cells were treated with a single dose of ITE (1 μM) up to 24 h. Samples of total mRNA were subjected to real time PCR. Protein and mRNA data normalized to GAPDH are expressed as Means ± SEM fold of the time 0 control (n = 3–5).*Differ from the time 0 control ($p \leq 0.05$).

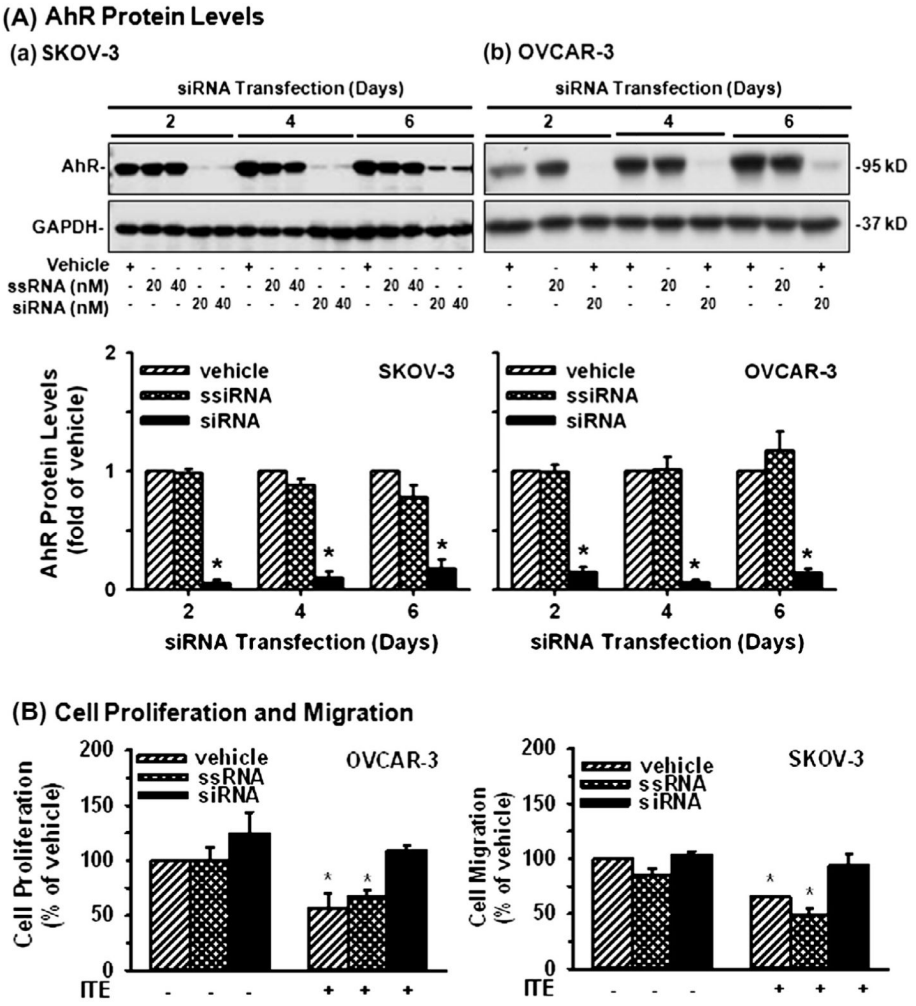

Fig. 5.

Effects of AhR knockdown on OVCAR-3 cell proliferation and SKOV-3 cell migration. (A) Cells were treated with the vehicle control, the scrambled siRNA (ssiRNA) or AhR siRNA (siRNA) up to 6 days. Proteins were subjected to Western blotting. Data from 20 nM siRNA treatments are present and expressed as Means ± SEM fold of the vehicle control ($n = 3$). (B and C) After siRNA transfection for 2 days, cells were treated with ITE (1 μM) for additional 4 days (for cell proliferation) or 2 days (for cell migration). Data are expressed as Means ± SEM% of the vehicle control ($n = 5–6$). *Differ from the vehicle control ($p \leq 0.05$).

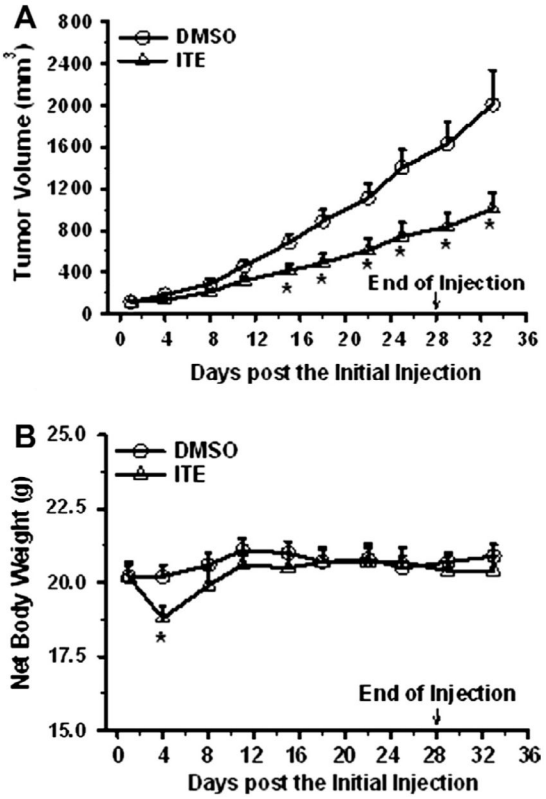

Fig. 6.

Effects of ITE on growth of OVCAR-3 cell xenografts in mice. OVCAR-3 cells were inoculated into mice. After formation of the tumor, the mice were injected with DMSO or ITE dissolved in DMSO daily for 28 days. Tumor volume and net mouse body weight were determined. Data are expressed as Means ± SEM (n = 8/group). *Differ from the DMSO control at each corresponding time point ($p \leq 0.05$).